Title
Theory of filamentation in relativistic electron beams

Permalink
https://escholarship.org/uc/item/0rj7c0zb

Journal
Physics of Plasmas, 15(6)

ISSN
1070-664X

Author
Benford, G

Publication Date
1973-06-01

DOI
10.1088/0032-1028/15/6/003

Peer reviewed

THEORY OF FILAMENTATION IN RELATIVISTIC ELECTRON BEAMS

G. BENFORD

Department of Physics, University of California, Irvine, Calif. 92664, U.S.A.

Abstract—Electron beams can be unstable to transverse modes which form small pinch structures, as first pointed out by Weibel. Beams which are not totally self-pinched are liable to this instability, so current neutralized regions near the beam head should display it. If the background response is nonresistive, filamentation is very rapid; if an axial magnetic field is present, interchange instability is competitive and the two may not be distinguishable. Beam motion is usually dominated by the resistive region, where $(\omega a/c)^2 \gg 1$, which we treat in detail. Using helical particle orbits in a uniform beam of radius a, we find the dispersion relation and growth rates in a number of differing cylindrical configurations. Because all particles have a common betatron frequency a sharp particle resonance appears, which may be broadened by energy spread in the beam. This model is most useful for beams in external axial magnetic fields, which are destabilised by electron drifts. We consider applications to experiment and methods of stabilisation.

1. INTRODUCTION

IT HAS long been known that streaming charged particles are unstable to the formation of local pinched current structures (WEIBEL, 1959). This is the "tearing" mode. It has been extensively investigated recently by LEE and ARMSTRONG (1971).

An electron beam propagating through a plasma should display this propensity to break up into small filaments. Simple arguments show that the configuration is marginally stable if the beam meets the BENNETT (1934) pinch condition (FURTH, 1963). For weaker pinching the beam is unstable. Pinching is retarded by plasma currents I_p in the background medium which can partially neutralize the beam current I_b, $I_p \approx - I_z$. The net v/γ of the beam governs suppression of filamentation, so that even high intensity electron beams may display this instability when they are partially current neutralized (SPENCE, ECKER and YONAS, 1969).

To illustrate with a simple example: take an infinite, homogeneous beam streaming with velocity v_0 through a plasma. The beam is charge neutralized by this plasma and also $n_p \approx n_b$, so their plasma frequencies ω_b and ω_p are approximately the same. One may easily show that the growth rate $i\omega$ for a Lorentzian transverse velocity distribution is

$$+i\omega = \left(\frac{\omega_p k_\perp v_0}{\sqrt{\omega_p^2 + k_\perp^2 c^2}} - k_\perp v_\perp \right) \tag{1}$$

where $k_\perp$ is the transverse wave number and we have assigned the beam a perpendicular temperature $\sim m v_\perp^2/2$. If $v_\perp > v_0$, stable standing waves exist. When $v_\perp < v_0$ there are always unstable long-wave length modes, with maximum growth rate

$$(i\omega)_{\max} = \frac{\omega_p}{c} (v_0^{2/3} - v_\perp^{2/3})^{3/2}. \tag{2}$$

We shall find throughout this paper that unstable modes are purely growing.

These results are non-relativistic, so we cannot take $v_0 \to c$ with confidence, yet the growth indicated by (2) is clearly large for sizable streaming velocities. In an actual beam $v_\perp$ arises because the beam self-field B_{θ_0} prevents simple outward movement of beam particles and instead pinches the beam radially. Equation (2) reflects the usual

Landau damping condition that growth is limited by the phase mixing which occurs when a thermal particle may move through an instability wave-length during one e-folding of the growth, $k_\perp v_\perp > i\omega$.

To proceed further, one must abandon simple models for the particle motion such as the above, and begin to include the effects of the beam self-field in a more realistic fashion. This paper treats a uniform beam of radius a, infinite along z within which electrons execute helical orbits due to the beam self-field, B_{θ_0}.

Since the betatron frequency of particles in the field of a uniform current J_b is independent of their perpendicular velocity, a uniformly coasting beam with constant current to some radius a will have one betatron frequency, ω_β. A resonance may be set up between this particle motion and a perturbed field, leading to enhanced growth which may only be treated by the Vlasov equation. In this resonant character our calculation differs from earlier work (FURTH, KILLEEN and ROSENBLUTH, 1963; WEINBERG, 1967). One would typically expect, using a hydrodynamic model, to find growth rates of order τ^{-1} where τ is the magnetic diffusion time, $4\pi\sigma a^2/c^2$, with σ the conductivity of the background plasma. Our results exceed this growth by a large factor which arises from resonant particle orbits. We also explore the effect of boundary conditions upon the growth of azimuthal perturbations $\sim e^{im\theta}$ for several different experimental configurations.

We assume the beam is of length $L_0 \gg a$, so a simple cylindrical equilibrium applies (BENFORD and BOOK, 1971). Throughout this length we take the beam self-field to be partially neutralized by plasma currents, so $v_z\tau \gg a$. We also assume long-wavelength perturbations along the axis, $k_z a \ll 1$. The dependence of the self-field upon distance behind the beam head will not be included explicitly, since this renders the boundary-value problem for the perturbed fields far more difficult. Since the beam betatron frequency ω_β changes over the length $v_z\tau$, we presume the radial dependence is more important in determining the rate of growth and its dependence on azimuthal wave number m. This restriction will be removed in a subsequent paper. We shall also ignore plasma particle motion beyond the effect of the induced return current, and ion dynamics; a brief comment on these matters appears in the final section.

Over all considerations of resistive beam modes hangs the possibility that rapidly growing non-resistive instabilities at the beam head may strongly determine subsequent beam motion. These aspects are discussed in Section 2. A simple beam model for the resistive regime which includes helical betatron orbits is described in Section 3. The model is applied to several different cylindrical configurations in the absence of an applied magnetic field B_{z0} in Section 4. We include B_{z0} in Section 5. In fact, our model applies best to this case since the electron drifts are well described by the helical orbit model. The special case of hose motion is treated in Section 6 and we indicate how the uniform beam density constraint used in Sections 3 and 4 may be relaxed in at least a qualitative manner.

These calculations apply most readily to the relativistic, high current electron beams now under extensive development. In Section 3 we decouple transverse and axial motion by assuming v_0 does not change appreciably during development of the instability. This will be true if the beam self-field is relatively weak for these times (current neutralization) or if the energy factor

$$\gamma = \left(1 - v_z^2/c^2 - \frac{v_\perp^2}{c^2}\right)^{-1/2}$$

greatly exceeds unity. We summarize by requiring that $v/\gamma \leq 1$, where v is the Budker parameter, modified to account for plasma currents I_p,

$$v = \frac{e^2}{m_e c^2} \left(1 - \frac{I_p}{I_b}\right) \int 2\pi r n_b(r) \, dr, \qquad (3)$$

so in the usual terminology we are speaking of the *net* v/γ.

2. THE NON-RESISTIVE MODES

The production of an intense relativistic beam in a field-emission diode is a complex process (ECKER, 1971). The degree of beam self-pinching while in the diode seems to depend upon the diode configuration, the presence of an imposed axial magnetic field, and probably other considerations as well.

Even when once free of the diode, the rise of plasma current at the beam front is a complex phenomenon, worthy of extensive analysis (PUTNAM, 1971) For example, during injection into neutral gas, induced plasma current depends strongly on the condition for electrostatic gas breakdown, and thus on gas pressure. Generally in neutral gas injection there will be a time before gas breakdown when the plasma conductivity will be low and the magnetic diffusion time τ will be quite short. This means currents can move readily through the plasma medium and any instability present is not of the resistive type. In this paper we shall denote the boundary between these regions by $(\omega a/c)^2 = 1$, or $v\tau = 1$, where v is the collision frequency used to determine conductivity in the background plasma. When $v\tau \ll 1$ instabilities are non-resistive; when $v\tau \gg 1$ the resistive time scale dominates motion. If the conductivity of the background rises in a time t_i, this defines a length of the beam $v_z t_i$ which exists in a non-resistive medium. In this regime the resistive filamentation instability will not occur because there will be no appreciable plasma currents induced by the rapid rise in magnetic field at the beam head. If the medium is already pre-ionized, of course, this non-resistive regime may be negligibly short. If not, the later evolution of filamentation may be significantly affected by the rapid growth of several instabilities in the non-resistive regime—notably non-resistive filamentation, the flute and the firehose.

Non-resistive filamentation is restrained by the rate at which the background neutralizing particles can move. Electrostatic fields arise when the beam electrons bunch, and if growth is to continue these fields must be neutralized by background charges. For early times, when the beam density n_b has been just barely compensated by n_I ions of mass m_i, all background plasma electrons are expelled from the beam volume and only the ions remain. During this stage, growth of non-resistive filamentation will be retarded by a factor $\sim \gamma m_e/m_i$, where m_e is the electron rest mass, since the ions are sluggish. As further ionization occurs, we expect the growth rate will increase until the problem of charge neutralizing the filamentary bunches becomes unimportant. The linear growth rate will remain fixed until the background plasma conductivity σ is large enough to necessitate treating the instability with a resistive model.

We can estimate the growth by taking a rippling perturbation on the surface of a cylindrical beam and calculating the perturbing force which arises from these ripples. The strength of the force depends, of course, upon the degree of current neutralization and the perturbation wavelength, $2\pi a/m$, where m is the azimuthal wave number. A simple Newton's law argument similar to that of FINKELSTEIN and STURROCK (1961) leads to

$$m_e \gamma \frac{d^2 r}{dt^2} \approx \frac{v}{\gamma} \frac{c^2 m}{\pi a^2} r \qquad (4)$$

for the motion of a small current filament on the surface of the beam. Equation (4) applies if $n_b \gg n_I$. For early times when $n_I \leq n_b$, the right hand side of this equation should be multiplied by $\gamma m_e/m_i$. The growth rate,

$$i\omega = \frac{c}{a} \sqrt{\frac{\nu}{\gamma} \frac{m}{\pi\gamma}} \tag{5}$$

is disastrously fast. Such an instability will produce wholesale filamentation while the beam is still in the diode, and, once exited, at the head of the beam as it propagates. It seems possible that the perturbation will be further enhanced if the fields form a standing wave in the open-ended 'cavity' of the diode, even though wave energy is being continuously convected out of the diode by the beam. The stabilizing effect of the nearby diode walls may help somewhat, but intuition suggests that large wave numbers m will remain unaffected until the perturbation wavelength is comparable to the distance between beam and diode walls.

Though (5) predicts larger growth for high m, these modes may never be realized in the diode because the severe gradients in density and field tend to smear out such detail in current structure. In the larger tank beyond the diode this argument may not hold. In a long chamber the final amplitude of modes as a function of m will probably depend upon non-linear effects which are difficult to estimate.

It seems profitable to reduce the maximum growth $i\omega$ by avoiding beams of small radius. Since what matters is the curvature, a hollow (annular) beam may thus prove quite useful in avoiding or ameliorating filamentation (BENFORD, BOOK and SUDAN, 1970).

When an applied magnetic field B_{z0} is present, new modes appear (i.e. interchange) and familiar ones are altered. Ignoring the self-field, we return to the description which gave the growth rate of (1) and find by a similar argument that maximum growth is approximately (for a cold beam)

$$i\omega \approx \sqrt{\omega_p{}^2 \left(\frac{v_0}{c}\right)^2 - \omega_c{}^2}.$$

This problem and similar situations has been more extensively treated by LEE (1970). Thus filamentation growth is reduced by an applied axial field, as we would expect, since current bunching across field lines is retarded. (This is not the case when electron drifts due to $B_{\theta0}$ are included; see Section 5.) But other modes are enhanced by a large axial field.

The interchange or "fluting" instability is a venerable and well-understood mode, in which dense plasma interchanges with the external magnetic field lines. Either the beam or background plasma may interchange with the field lines. The appropriate growth rate follows from the general form given by LONGMIRE (1963),

$$i\omega = \pi k_z \sqrt{\frac{mp}{\rho}}$$

where p is the pressure and ρ the mass density of the fluting plasma.

For a beam injected into a gas, before gas breakdown (and thus before high levels of plasma ionization are attained) the beam may interchange with the field provided it can drag along background ions, so

$$i\omega = \pi k_z v_z \sqrt{\frac{mm_e}{2m_i}} \, \nu. \tag{6}$$

After breakdown, the sluggishness of the dense background plasma lowers this growth rate by a factor of $(n_p/n_b)^{1/2}$.

One might expect, then, that fluting will occur quickly before breakdown and observed damage patterns will depend on the initial features of the beam. Indeed, if the gas is pre-ionized, interchange will occur in the plasma before the beam is injected, so that a fluted field pattern then guides the beam and ripples on the beam surface are observed downstream. These fossils from before injection may readily be mistaken for beam fluting itself.

Note that the growth rates above are independent of applied field B_{z0} and show the usual $m^{1/2}$ dependence. For most intense beam experiments a growth length $\sim$ meter results. Fluting may not be easily distinguishable from resistive filamentation in an external field (see Section 5), but generally it will produce beam motion preferentially at the beam *edge*, whereas filamentary structure may form throughout the beam *area*. This may not be a particularly useful rule, however, in analysing experiments, since nature seldom presents one with clear patterns from which modes may be deduced. Perhaps in a particular situation enough parameters can be varied (σ, B_{z0}, ν/γ) to distinguish between the growth rate of (6) and those of Section 5. Without an applied field, of course, interchange instability does not occur and filamentation leaves a clear signature.

The firehose ($m = 1$) mode will also proceed rapidly, as pointed out by FINKELSTEIN and STUR-ROCK, in the non-resistive regime. Such sidewise movement will quickly destroy beam focusing. The mode occurs when

$$n_b m_e \gamma v_0^2 \left(\gamma^2 - \frac{\nu}{\gamma} \right) \geq \frac{B_{z0}^2}{2\pi}.$$

(7)

In general, the rapid development of transverse instabilities in the non-resistive region will erode the beam front as it passes through a neutral gas, in addition to losses from the region at the head in which charge neutralization is taking place. Growth in the non-resistive region near the beam head may well serve to initiate filamentation in following portions of the beam when the resistive instability is dominant ($v_0 \tau \gg a$), so that filaments do not develop from random background noise. In addition, there may be asymmetric features in the walls (such as strips of higher conductivity to encourage return currents) or in the beam current itself, which arise from particular facets of the experiment.

Also, rapid onset of high conductivity (such as that due to rapid heating through ion-acoustic modes) may "freeze" a non-resistive mode throughout the rest of the beam pulse, so that one observes a fossil of the early time behavior of the transverse instabilities. "Frozen" hose motion particularly seems commonly observed (BENFORD, private communication); evidence of fluting may have the same early time origin. In practice it may be difficult to distinguish between "frozen" fluting and later development of resistive filamentation when beams are propagated in neutral gases.

All these caveats imply that the non-resistive regime at the very front edge of a beam is not susceptible to easy analysis, particularly given the theorist's professional addiction to simple models. Luckily, the most interesting applications for relativistic electron beams (plasma heating, ion acceleration, etc.) arise when beams are injected into at least partially pre-ionized media, so that the non-resistive region is quite small. We shall therefore neglect it, except to note that current fluctuations therein may give substantial perturbations to the resistive regime which dominates beam behavior behind the head.

3. BEAM MODEL FOR RESISTIVE FILAMENTATION

Since we contemplate describing the influence of cylindrical boundary conditions on filamentation, we should pick a simple beam equilibrium to avoid having to follow complex individual particle motions. The electrons execute betatron orbits in the beam self-field and as we shall see, resonance in this motion governs the magnitude of the maximum growth rate.

We shall consider beam electrons which move in circular helices. Thus they feel a simple harmonic force when the current density is uniform to some radius a (as we shall assume) and their betatron frequencies are independent of r. To take any more complicated unperturbed particle orbits would introduce at least one second order differential equation, aside from Maxwell's equations, and would considerably obscure the physics (MJOLSNESS, 1963). To decouple axial and transverse motion we do not allow the axial beam velocity v_z or radius a to change while filamentation takes place, so beam current I_b is constant. In this approximation the electrons have two transverse constants of the motion as well,

$$2E = \left(\frac{dr}{dt} \right)^2 + v_\theta^2 + \omega_\beta^2 r^2$$

(8)

$$M = r v_\theta$$

where $v_\theta = r \, d\theta/dt$. The betatron frequency in the beam self-field is

$$\omega_{\beta o} = \sqrt{\frac{2ev_z I_b}{\gamma m_e c^2 a^2}} = \sqrt{\frac{\omega_b^2}{2} \left(\frac{v_z}{c}\right)^2} \tag{9}$$

where ω_b is the beam plasma frequency. Since the electrons have circular orbits, dr/dt is zero and ω_{β_0} is constant.

We can write the equilibrium distribution function for our uniformly coasting beam in several ways, depending upon which problem we wish to treat. In Section 5 we shall use the uniform density equilibrium to describe electron orbits in an imposed field B_{z0}, in which case ω_β will be replaced by a net particle drift frequency and f_0 will be uneven in v_θ. Though we could exclude explicit dependence on either ω_β or E from f_0, we shall find it convenient to use both variables. In a magnetic field a uniform density equilibrium with circular drift orbits is clearly satisfactory. Recently LEARY and LEE (1972) have demonstrated a whole class of low v/γ equilibria, in particular a uniform density case

$$f_0 = \frac{2n_b S(\omega_\beta) \, \delta(v_z - v_0)}{\pi \gamma \omega_\beta r^2 a^2} \, \delta \left(\frac{mc^2 \gamma \omega_\beta^2}{2v_z I_b} - \frac{cA_{z0}^{(r)}}{I_b r^2} - \frac{1}{r^2} \right)$$

where $S(\omega_\beta)$ is the distribution in betatron frequencies, and $A_{z0}(r)$ is the vector potential (z component). The uniform density model has also been used by WEINBERG (1961).

Filamentation occurs most readily when there is little beam self-field present. We must remember that the region near the front of a relativistic beam is subject to considerable inbalance of radial forces. Without an applied axial field, the current neutralization at the beam head leads to radial blowup. The beam electrons there, if they are confined at all, execute orbits with low betatron frequencies. This will be the case until filamentation generates a substantial level of small, self-pinched regions with appreciable self-field. By this time the linearized Vlasov theory we use no longer applies, since the equilibrium described by $f_0(E, M, \omega_\beta)$ will have been considerably perturbed. Near the beam head the betatron frequency is not the equilibrium value given by equation (9), but rather

$$\omega_\beta = \sqrt{\frac{2ev_z}{\gamma m_e c^2 a^2} (I_b - I_p)} \tag{10}$$

where I_p is the current induced in the background plasma by the changing magnetic field at the beam front. With good current neutralization, $I_z = I_b(1 - e^{-\xi/v_0\tau})$, where ξ is the distance back from the beam front and τ the magnetic diffusion time. Clearly $\omega_\beta \ll \omega_{\beta_0}$ throughout the region of interest for the filamentation instability.

Assuming that $v_z\tau \ll a$, $v_\perp \ll v_z$ (so that perpendicular and parallel perturbations do not couple), and $k_z a \ll 1$ (long wavelength approximation along z), we consider a uniform electron beam infinite along z but of finite radius a, which undergoes filamentation while its self-field is partially neutralized by plasma currents. The scattering of beam electrons by the background plasma is neglected and this plasma is described solely by a conductivity σ. Streaming instabilities and the sausage mode ($m = 0$) are not treated. Though our beam profile is rectangular, this restriction is not significant and the effects of relaxing it will be discussed qualitatively in Section 6.

The Vlasov equation for the perturbed distribution $f_1(r, v_z, v_\theta, t, \omega_\beta)$ is

$$\left(\frac{\partial}{\partial t} + \mathbf{v}_\perp \cdot \frac{\partial}{\partial \mathbf{r}_\perp} + v_z \frac{\partial}{\partial z}\right) f_1 - \frac{e}{\gamma m_e c} (\mathbf{v}_z \times \mathbf{B}_0) \cdot \frac{\partial f_1}{\partial \mathbf{v}_\perp} - \frac{e}{\gamma m_e c} (\mathbf{v}_z \times \mathbf{B}) \cdot \frac{\partial f_0}{\partial \mathbf{v}_\perp} = 0. \quad (11)$$

Here $\mathbf{B}$ is the perturbed field, which has components B_θ and B_r. We shall find it easier to deal with the vector potential A_z. The formal solution of (11) follows by integrating over our helical particle orbits discussed earlier,

$$f_1 = \frac{e}{\gamma m_e c} \int_{-\infty}^t dt' \left[\mathbf{v}_z \times \mathbf{B} \cdot \frac{\partial f_0}{\partial \mathbf{v}_\perp}\right]_{\text{orbit}}. \quad (12)$$

The advantage of helical orbits is that

$$\frac{\partial f_0}{\partial \mathbf{v}_\perp} = \frac{\mathbf{v}_\theta}{|\mathbf{v}_\theta|} \frac{\partial f_0}{\partial v_\theta} = \frac{\mathbf{v}_\theta}{|\mathbf{v}_\theta|} \left(\frac{2M}{r} \frac{\partial f_0}{\partial E} + r \frac{\partial f_0}{\partial M}\right)$$

which is constant along a particle orbit, so we can take it outside the integral in (12). We now Fourier analyse, $f_1, A_z \sim e^{i(m\theta + kz - \omega t)}$ and integrate over time. The perturbed current is then

$$J_{1z} = -e \int_0^\infty d\omega_\beta \int d\mathbf{v} f_1 v_z = \frac{eca^2}{2I_b} \frac{A_z}{r} \int_0^\infty \omega_\beta^2 \, d\omega_\beta \int d\mathbf{v}$$

$$v_z \frac{\left(\dfrac{2M}{r} \dfrac{\partial f_0}{\partial E} + \dfrac{r}{\partial M} \dfrac{\partial f_0}{\partial M}\right)}{\dfrac{mv_\theta}{r} - (\omega - kv_z)} \quad (13)$$

For the $B_{z0} = 0$ case of Section 4, where the orbits are indeed betatron orbits, Lee has pointed out (private communication) that a higher order treatment of the transverse perturbation than that given here is necessary if one desires the very high frequency response and growth rates. However, this is not true of the axial field model, Section 5, since the circular orbits used are drift orbits, and do not perturb easily transversely as do ordinary betatron orbits. The results of Section 5, which are the principal results of this paper, remain so long as the perturbation frequency does not exceed the beam cyclotron frequency in the applied magnetic field.

The dispersion relation is found by using Maxwell's equation,

$$\left(\frac{1}{r} \frac{\partial}{\partial r} r \frac{\partial}{\partial r} - \frac{m^2}{r^2} + \frac{4\pi i \sigma \omega}{c^2}\right) A_z = -\frac{4\pi}{c} J_{1z}. \quad (14)$$

We shall first consider cases with no axial magnetic field B_{z0}, for which the helical particle orbits are a fair approximation.

4. NO AXIAL MAGNETIC FIELD

In the absence of an external field the beam will not rotate, so $f_0(v_\theta)$ is even in v_θ. The perturbed current J_{1z} may be written

$$J_{1z} = \frac{e^2 v_0^2}{m_e \gamma c} \int d\omega_\beta \int dv_\theta \frac{\dfrac{\partial f_0}{\partial v_\theta} \dfrac{mv_\theta}{r}}{\left(\dfrac{mv_\theta}{r}\right)^2 - (\omega - kv_z)^2}. \quad (15)$$

Using the constants of the motion M and E, we have

$$\frac{\partial f_0}{\partial v_\theta}\frac{v_\theta}{r} = \left(r\frac{\partial f_0}{\partial M} + \frac{2M}{r}\frac{\partial f_0}{\partial E}\right)\frac{M}{r^2} = \frac{\partial f_0}{\partial M}\frac{\partial M}{\partial r} + \frac{\partial f_0}{\partial E}\frac{\partial E}{\partial r} = \frac{\partial f_0}{\partial r}. \tag{16}$$

For a beam of constant density n_0 to radius a, $\partial f_0/\partial r \sim \delta(r-a)$. Such a sharp dependence on r leads to a simple boundary value problem for A_z. Had we assumed a more reasonable beam shape—say, a Gaussian or Bennett form—A_z would be given by the solution to a rather difficult differential equation. To display our results with a minimum of complication we shall assume the square beam profile and comment upon other profiles in Section 6. We shall also take f_0 separable in ω_β, and all electrons coasting uniformly along the z-axis, so that

$$f_0 = f_0(M, E)S(\omega_\beta)\,\delta(v_z - v_0) \tag{17}$$

where

$$\int_0^\infty S(\omega_\beta)\,d\omega_\beta = 1.$$

Our equation for A_z follows from (13), (14) and (17):

$$\frac{1}{r}\frac{\partial}{\partial r}r\frac{\partial}{\partial r}A_z - \frac{m^2}{r^2}A_z + \frac{4\pi i\sigma\omega}{c^2}A_z = -2\frac{\delta(r-a)}{a}h_m A_z \tag{18}$$

where

$$h_m = \int_0^\infty d\omega_\beta S(\omega_\beta)\frac{(m\omega_\beta)^2}{(m\omega_\beta)^2 - (\omega - kv_0)^2} \tag{19}$$

is the average of the resonant denominator over the beam energy spread.

The resonant denominator in h_m is large when the Doppler-shifted frequency of the perturbation, $\omega\text{-}kv_0$, equals $m\omega_\beta$. A portion of the beam electron population experiences a constant driving electric field and the instability is disastrous. This effect is partially a result of our simple model, in which all electrons move harmonically. In an actual beam a perturbing field will act upon electrons which have differing ω_β because of a velocity spread in v_z, because $J_b(r)$ is not uniform, or because transverse and longitudinal motion are not completely decoupled. To allow for this we represent the energy spread of the beam by $S(\omega_\beta)$, which will be peaked in some fashion with width $\delta\omega_\beta$, so that $\omega\text{-}kv_0 \approx m(\omega_\beta \pm \delta\omega_\beta)$. Since we do not know $S(\omega_\beta)$ (though in specific experiments such information may be available) we replace the integration over ω_β with the average frequency spread; this fixes the magnitude of wave growth. Within this approximation we find h_m is independent of m,

$$h_m = \frac{\omega_\beta^2}{2\omega_\beta\,\delta\omega_\beta}. \tag{20}$$

We consider a general boundary value problem as depicted in Fig. 1. The beam of radius a is surrounded by a plasma channel of constant conductivity σ and radius R. Further away at L a pipe of infinite conductivity forces the axial electric field to zero. We require that A_z be well behaved at the origin, vanish at L and have a continuous logarithmic derivative at the channel boundary:

$$\frac{1}{A_z(m)}\frac{\partial A_z(m)}{\partial r}\bigg|_{r=R} = -\frac{m}{R}. \tag{21}$$
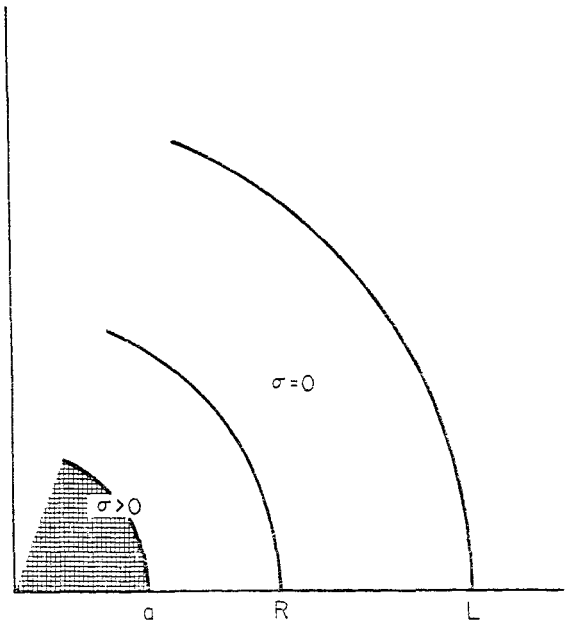
FIG. 1.—A cylindrical beam of radius a in a conducting channel of radius R, with a conducting wall at L.

We shall scale (18) in the parameters

$$x^2 = -i\omega\tau \qquad \tau = \frac{4\pi\sigma a^2}{c^2} . \tag{22}$$

On either side of the point $r = a$, (18) has the form of Bessel's equation. We may use the above continuity conditions to connect the solutions across $r = R$. A_z is continuous at $r = a$. By integrating (18) across $r = a$ we can obtain one final condition on the fields. The dispersion relation so obtained is expressed in terms of the modified Bessel functions

$$I_n(y) \underset{y\to 0}{\longrightarrow} \frac{y^n}{2^n\Gamma(n+1)}$$

$$K_n(y) \underset{y\to\infty}{\longrightarrow} \sqrt{\frac{\pi}{2y}}\, e^{-y}. \tag{23}$$

We consider several special configurations.

(a) $R > a, L \to \infty$

This represents an ionized channel surrounded by gas to large radii. Application of the boundary conditions leads to the dispersion relation

$$1 = 2h_m F_m(x) \tag{24}$$

with

$$F_m(x) = I_m(x)\left[\frac{K_m(x)}{I_m(x)} + \frac{K_{m-1}\left(\dfrac{xR}{a}\right)}{I_{m-1}\left(\dfrac{xR}{a}\right)}\right]. \tag{25}$$

We anticipate that the growth rate $i\omega$ will be faster than the diffusion rate τ^{-1} and thus

expand the dispersion relation for $x \gg 1$,

$$F_m(x) \cong \frac{1}{2x}\left\{1 - \frac{9m^2}{16x^2} + e^{2x(1-R/a)}\left[1 - \frac{m^2}{x}\left(1 - \frac{a}{R}\right)\right]\right\}. \tag{26}$$

We have assumed $x \gg m^2$ and expanded in m^2/x.
If $R \gg a$ we find

$$x \approx h_m\left(1 - \frac{9}{16}\frac{m^2}{h_m^2}\right). \tag{27}$$

The growth rate falls off with higher m when we can insure that h_m is independent of m. For a beam which nearly fills its channel we write $R/a = 1 + \varepsilon$ and find

$$x \approx h_m\left(1 - \frac{9}{16}\frac{m^2}{h_m^2}\right) + h_m e^{-2\varepsilon h_m}e^{9\varepsilon m^2/8h_m}. \tag{28}$$

Within these approximations x has a minimum at

$$m_{\min} \cong \tfrac{4}{3}h_m\sqrt{1 + \frac{\ln 2\varepsilon h_m}{2\varepsilon h_m}}. \tag{29}$$

For a sharp beam energy distribution $h_m \gg 1$ and $m_{\min}$ may represent very fine-scale transverse structure indeed. As is indicated schematically in Fig. 2, for $L \gg R$ growth may be large for both high and low m-values, but for $m_{\min} \gg 1$ probably only the low values could be observed experimentally.

(b) $L = R > a$

This represents the common case wherein the conducting background plasma extends to the containing walls. The dispersion relation has the same form as (24), with

$$F_m(x) = I_m^2(x)\left[\frac{K_m(x)}{I_m(x)} - \frac{K_m\left(\dfrac{xR}{a}\right)}{I_m\left(\dfrac{xR}{a}\right)}\right]. \tag{30}$$
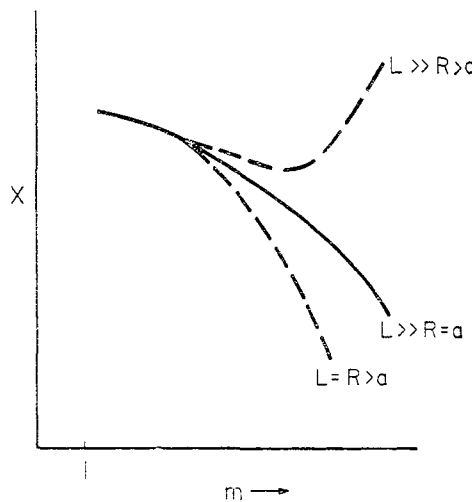

FIG. 2.—Schematic view of growth parameter $x = (i\omega\tau)^{1/2}$ as a function of azimuthal mode number m for different cylindrical configurations.

For large m such that $m - 1 \approx m$ we can simply change the sign before the exponential term in (26) in order to find solutions with $x \gg 1$. The result (27) holds as well, and by changing the sign of the second term in (28) we find a somewhat better expression for the m- dependence of x in this case. With this change, x no longer has a minimum in m, but instead declines monotonically (see Fig. 2).

(c) $L \to \infty$. $R < a$

This case is appropriate to very early times in a beam pulse, when a narrow channel has been formed but beam expansion at the head has allowed some fraction of the beam electrons to move radially into the nearby volume of low conductivity. Instead of solving the problem with two regions of differing but finite conductivity, we shall take $\sigma \neq 0$ inside R $(\lesssim a)$ and zero elsewhere. Elements of the beam in regions of low conductivity are subject to non-resistive instabilities, such as the firehose, which are very rapid, as noted earlier. For our purposes we shall assume they are stabilized or otherwise negligible; that is, the outer conductivity is not too low. This very simple model yields the dispersion relation

$$1 = \frac{h_m}{m} \left\{ \left(\frac{R}{a}\right)^{2m} \left(\frac{\dfrac{ma}{R} - \dfrac{I_m'\left(\frac{xR}{a}\right)}{I_m\left(\frac{xR}{a}\right)}}{\dfrac{ma}{R} + \dfrac{I_m'\left(\frac{xR}{a}\right)}{I_m\left(\frac{xR}{a}\right)}} \right) - 1 \right\} \tag{31}$$

where

$$I_m'(y) = \frac{dI_m(y)}{dy}$$

This equation yields growth rates

$$x \sim h_m \left(\frac{R}{a}\right)^2.$$

as one would expect, since proportionally less of the beam participates. For $r > R$, of course, the growth rates of Section 2 apply, and can be much more rapid. Realistically, non-resistive features will dominate for such early times.

(d) The annular beam

Confining a beam between two concentric metal cylinders is useful for focusing and concentration, particularly when the cylinders are tapered into a cone. The dispersion relation for such a case, with tapering, is quite complicated. Removal of the z-dependence (no tapering) still presents a formidable problem and only special cases may be readily solved. The simplest is an annular beam with inner radius d, outer radius a, and both the inner and outer conducting cylinders far away. Ignoring these stabilizing boundaries probably overestimates slightly the growth for filamentation, at least for low values of m. The dispersion relation may be cast into the form

of (24), with

$$F_m = K_m(x) \left[I_m(x) - \frac{K_m(x) I_m{}^2\left(\dfrac{xd}{a}\right)}{K_m\left(\dfrac{xd}{a}\right) I_m\left(\dfrac{xd}{a}\right) + \dfrac{a}{2dh_m}} \right]. \tag{32}$$

Expanding for $x \gg m^2$,

$$x \cong - \frac{\ln\left(1 - \dfrac{x^2}{h_m{}^2}\right)}{2\left(1 - \dfrac{d}{a}\right)}. \tag{33}$$

Writing $1 - d/a = \delta \ll 1$ for a thin annular beam and working out the first order dependence on m, maximum growth is given by

$$x \approx 2\delta\left(h_m{}^2 + \frac{m^2}{1 - \delta}\right). \tag{34}$$

In contrast with the $L \gg R$, $\epsilon > 0$ result, there is no minimum in x as m increases. Higher order terms would doubtless reveal more information. But since for this configuration we expect from physical intuition the most rapidly growing mode to have

$$m \gtrsim \frac{a}{a - d} \gg 1, \tag{35}$$

expansion in m^2/x is not a good procedure and the dispersion relation becomes far less transparent. Our model is perhaps less convincing for this annular case, too, since particle orbits seem unlikely to wrap neatly around the large circle rather than bouncing across the narrow gap of width a-d. As we shall see in the next section, an applied field B_{z0} does so constrain the electrons to drift around in large circles, so these results will seem more reasonable in that context.

5. APPLIED AXIAL FIELD

The most obvious agent for directing and containing an otherwise recalcitrant electron beam is an imposed axial field which dominates the beam self-field, $B_{z0} \gg B_{\theta 0}$. Precisely how strong B_{z0} must be to contain a beam with high transverse pressure is not yet quite clear. The critical field appears to depend upon details of the diode design and injection conditions (ECKER, 1971), and it seems the qualitative guess $B_{z0}{}^2 > \gamma m/2$ $v_\perp{}^2$, which follows from a simple pressure balance argument, is an overestimate. It is clear, though, that the condition $\omega_c \gg \omega_\beta$ must hold, where ω_c is $eB_{z0}/m\gamma c$. In such a case the beam electrons undergo two types of motion: rapid cyclotron orbits with small cyclotron radii, and a slower rotation about the beam axis at frequency (BENFORD, 1972).

$$\bar{\omega} \cong \frac{\omega_\beta{}^2}{\omega_c} = \frac{2\pi n_b ec}{B_{z0}} \left(\frac{v_z}{c}\right)^2 \left(1 - \frac{I_p}{I_b}\right). \tag{36}$$

It is interesting to note that for a relativistic beam ($v_z \approx c$), $\bar{\omega}$ is very nearly independent of particle energy. The broadening of the resonance which we encountered in (20) will not occur, then, for the drift rotation $\bar{\omega}$. We can easily carry over our helical

electron orbits for this case with assurance, since the electrons do drift around the beam center (HAMMER and ROSTOKER, 1970) at frequency $\bar{\omega}$ when $\omega_c \gg \omega_\beta$. The beam has a net angular momentum and $\partial f/\partial v_\theta$ is antisymmetric. Returning to equations (13) and (14), we retrace the steps of Section 4 to find that the same differential equation results, equation (18), but with h_m replaced by

$$g_m = m\omega_\beta^2 \int \frac{d\bar{\omega} S_B(\bar{\omega})\bar{\omega}^{-1}}{m\bar{\omega} - (\omega - kv_0)} . \tag{37}$$

The resonance in g_m is not as strong as the quadratic form of h_m, but on the other hand the distribution in drift frequencies, $S_B(\bar{\omega})$, must be a far more strongly peaked function than $S(\omega_\beta)$. $S_B(\bar{\omega})$ reflects the spread in $\bar{\omega}$ throughout the beam which arises from inhomogeneities in B_{z_0} and only weakly through energy spread, as remarked above. Using arguments similar to those which led to (20), we write

$$g_m = \frac{\omega_\beta^2}{\bar{\omega}\delta\bar{\omega}} . \tag{38}$$

The values of g_m and h_m due to energy spread $m_e c^2 \delta\gamma$ are

$$g_m{}^E = \left(\frac{\omega_\beta}{\bar{\omega}}\right)^2 \frac{\gamma^3\left(1 - \frac{1}{\gamma^2}\right)}{2\delta\gamma} \tag{39}$$

$$h_m{}^E = \frac{\gamma}{\delta\gamma} \tag{40}$$

so that

$$\frac{g_m{}^E}{h_m{}^E} = \left(\frac{\omega_c}{\omega_\beta}\right)^2 \frac{\gamma^2}{2}\left(1 - \frac{1}{\gamma^2}\right) \gg 1 . \tag{41}$$

On the other hand,

$$\frac{\delta\bar{\omega}}{\bar{\omega}} = \frac{\delta B_{z0}}{B_{z0}} - \frac{2}{\gamma^2\left(1 - \frac{1}{\gamma^2}\right)} \frac{\delta\gamma}{\gamma} \approx \frac{\delta B_{z0}}{B_{z0}} \tag{42}$$

for $\gamma \gg 1$.

Deviations of $B_{\theta0}$ from that given by a uniform current should be small, so probably $\delta B_{z0}/B_{z0}(\leq 10^{-1})$ is the major contributor to the resonance width g_m. Thus we expect very rapid growth indeed.

The maximum growth rates of Section 4 will still hold when an external field B_{z0} is imposed in the geometries considered, with g_m substituted for h_m. Indeed, the helical orbit model applies quite well for the electron drift (rotation) and is a more appealing simplification in this case than it is for the usual beam betatron orbits.

Thus, without further labor, we carry over our earlier work to the case of $B_{z0} \gg B_{\theta0}$. This fact is a major reason why we chose the simple helical orbits. Since most high intensity electron beam experiments use a strong axial field, the adapted equations of Section 4 are probably the most important results of this paper.

One intuitively expects that imposition of a strong axial field B_{z0} would retard transverse beam motion, as mentioned in Section 2. This would surely be so but for

the drift of electrons at frequency $\bar{\omega}$, which is severely destabilising. Without this drift the helical orbits we have used would be wholly inappropriate and we would find appreciable transverse motion only through collisions, which we have hitherto neglected. The sharpness of the resonance in g_m implies that, should filamentation not be observed in field-free cases, it may appear when B_{z0} is applied.

6. HOSE MOTION

The $m = 1$ mode is a topic now hoary with age in plasma physics (ROSENBLUTH, 1960). We can particularize (24) to this case and find, as expected, that there is a solution $x = 0$ for $\omega - kv_0 \to 0$. This is simply a rigid displacement of the beam which does not change the energy. For $\omega_\beta^2 \gg (\omega - kv_0)^2$ the dispersion relation is

$$1 \approx F_1 \left(1 + \frac{(\omega - kv_0)^2}{\overline{\omega_\beta}^2} \right) \tag{43}$$

where $\overline{\omega_\beta}^2$ is the average over $S(\omega_\beta)$. The growth is

$$x^2 \cong \frac{(\omega - kv_0)^2}{\overline{\omega_\beta}^2} \frac{2}{\left(\ln \dfrac{R}{a} + \tfrac{1}{4} \right)} . \tag{44}$$

The log term is the familiar geometric factor in the diffusion time. Similar geometric terms appear in the different boundary condition problems considered in Sections 4 and 5.

For faster growth we find the maximum rates of Section 4 with $m = 1$, $x \approx h_1$. This strong resonance for $-i\omega$,

$$-i\omega \approx \tau^{-1} \left[\frac{\omega_\beta^2}{\omega_\beta^2 - (\omega - kv_0)^2} \right]^2 \tag{45}$$

seems somewhat mysterious, as we shall show. One could construct a simple theory for hose motion by writing the force law for both the beam and the plasma. Consider a beam undergoing transverse displacement y. The source of resistive hose instability is the inability of the beam's magnetic field to rigidly follow beam motion, since the field is constrained to move in times comparable to the diffusion time τ. Denote the position of the magnetic field axis by b. Then we expect the beam to obey a force equation

$$\frac{d^2 y}{dt^2} + \omega_\beta^2 (y - b) = 0 \tag{46}$$

which states that the beam oscillates at the betatron frequency about the field axis. If b was constant in time there would be no instability, only harmonic beam motion. The field axis attempts to join the beam axis, but must move in a dipolar manner, on a time scale τ,

$$\frac{\partial b}{\partial t} + \frac{1}{\tau} (b - y) = 0. \tag{47}$$

These two equations yield growth,

$$-i\omega = \frac{1}{\tau} \frac{(\omega - kv_0)^2}{\omega_\beta^2 - (\omega - kv_0)^2} . \tag{48}$$

This resonant denominator is not as strong as that of (45), which we have obtained with a uniform beam model. One naturally wonders if the constraint of a sharp beam profile, $\partial f_0 / \partial r \sim \delta(r - a)$ explains the difference. LEE (Lawrence Livermore Laboratory, private communication) has investigated this problem by considering a beam with a Gaussian profile in density. The root of the difficulty is that elements of current near the edge of a sharp-profile beam can undergo decay in a very short time, since currents need only diffuse a short distance. The simple result above, (48), ignored such effects and thus found a resonance less sharp than (45). Lee found that a beam with $n_b(r) \sim e^{-r^2/a^2}$ gave the same form of the resonance as (48). Extensive analysis of the Gaussian profile for $m > 1$ is a formidable task, however, and rather than pursue it we simply suggest that, since the mechanism which sharpened the hose resonance seems to apply to filamentation as well, we can account for it fairly well by replacing x by x^2 in the results of Section 4 and 5. This is only an approximate way to modify our results, of course, since abandonment of the uniform beam profile makes ω_β vary with radius. While an applied B_{z0} will tend to make a beam keep a square profile if it is injected with one, we must realistically expect significant deviations from uniform $J_b(r)$, especially if B_{z0} is weak. Relatively few electrons should be required to smooth the beam shape so that the resonant form of (48) applies, though. One intuitively expects the dependence on mode number m to be insensitive to the precise radial profile, since it results from boundary conditions at R and L as well.

The rate of growth, however, clearly is sensitive. If a sharp radial profile beam is injected into a plasma, the first effect of instability should be rapid filamentation near the boundary, smearing of the profile and a subsequent slower growth. This process cannot be described with the infinitesimal perturbation approach we have used.

Similarly, one might ask what will be the result of an exceptionally sharp distribution of beam betatron frequencies, so that h_m or g_m becomes very large. Then the beam energy distribution will be quickly altered by filamentary perturbations (as well as others, such as the electron–electron two stream instability) and the resonant character quickly smeared. Since most beams in practice are not monochromatic values of h_m or $g_m > 100$ seem unlikely, though.

7. CONCLUDING REMARKS

After noting in Part 2 the rapid growth of the non-resistive modes which can serve to initiate filamentation, we have subsequently pursued the conventional linear Vlasov treatment of the resistive mode. This ignores the possibility that filamentation may have proceeded beyond linear analysis even before the resistive regime is reached. This, as well as details of the diode design, may augment a particular value of m (or a family of m-values) and render useless our expectations of growth as a function of m. Of course if the simple model we have used (helical orbits, uniform density) applies to a beam while in the diode, we may expect from symmetry that the same functional dependence on m of the growth rates might apply, though not the magnitude of growth.

Resistive filamentation should be most readily observed in beams for which the pulse length is less than $v_0 \tau$. This means either short pulses or high conductivity in the background plasma. If the beam pinches down appreciably during the pulse, Landau damping will occur when

$$\mathbf{k} \cdot \Delta \mathbf{v} = \frac{m}{a} v_\perp + k \Delta v_z > \text{growth rate}$$

For a highly relativistic beam ($\gamma \gg 1$),

$$\Delta v_z \approx \frac{1}{2}\frac{v_\perp^{\,2}}{c}$$

and is quite small, but for most present experiments with high current, $\gamma \lesssim 3$. In the absence of B_{z0}, Landau damping requires

$$(m\omega_\beta + k\Delta v_z)\tau \gg h_m \tag{49}$$

and we stress that ω_β is the *local* betatron frequency, as given in (10). With $B_{z0} \gg B_{\theta 0}$, the requirement is

$$\left(\frac{mv_\perp}{a} + k\Delta v_z\right)\tau \gg g_m. \tag{50}$$

Thus high values of m are suppressed most readily as pinching begins. Since these modes have the most rapid growth in the non-resistive region (and also for the resistive case when $L \gg R$), they may at times be found in damage patterns near the diode but not further away. (This behavior—lower azimuthal numbers observed further downstream—may also occur from non-linear effects, since the tearing instability tends to select longer wavelengths after long times.) Also, if an appreciable fraction of the beam length does pinch, filamentary structures may be obliterated on a damage plate by the later portion of the pulse. We have found growth rates in time for a fixed laboratory coordinate. This may also be viewed as the growth of a filamentary pattern from head to tail of a beam pulse. Since ω_β varies behind the beam head, the growth length is not readily calculated. An average for a growth length would be of the form

$$l = \int_0^\infty \frac{d\xi}{i\omega(\xi)\tau}$$

and the dependence of $i\omega$ on ξ has been neglected in this paper. (It will be the subject of a future work.)

We have included return current in the plasma implicitly by using the ω_β appropriate for partial current neutralization, rather than $\omega_{\beta 0}$. It is worth noting that dynamic aspects of plasma particle motion beyond this will not come into play importantly unless the plasma is tenuous, $n_p \lesssim n_b$. This is valid shortly before charge neutralization is accomplished, but current neutralization will not have occurred because the plasma electrons will not have had time to be accelerated to $v_0 \approx c$. Thus the beam electrons will still be pinched and transverse instabilities will be suppressed, as indicated by equations (49) and (50). The motion of plasma ions has little effect on the maximum growth rates considered here as long as plasma density is high, $\gamma m_e n_p \gg n_b m_i$, since then charge perturbations are neutralized by plasma electrons alone. Ion motion can extend the filamentation instability to higher values of $k_\perp$, but the height of the peak in growth, which comes at lower values of $k_\perp$, remains unaffected (LEE, 1971).

Recently workers at several laboratories have observed filamentary structures which may be due to resistive modes. (C. STALLINGS, Physics International Company; D. HAMMER, Naval Research Laboratory; A. J. TOEPFER, Sandia Laboratories; all by private communication.) Sheet beams particularly may be expected to show filaments

easily, with growth rates as given earlier, to within geometrical factors of order unity. The same is true of the annular configuration discussed in Section 4 and 5.

The eventual importance of the filamentation instability may lie primarily in the possibility of non-linear coupling between higher m-numbers and the hose, $m = 1$. This will lead to sidewise motion and eventual loss of the beam. The beam may spray outward into several filaments. Such motion may be observed in time-integrated photographs from alongside the beam. As well, concentration of the beam into current structures $\sim a/m$, $m \gg 1$ can appreciably alter the heating properties of high current beams, with important implications for fusion applications.

REFERENCES

BENFORD G. and BOOK D. L. (1971) *Advances in Plasma Physics* (Edited by A. Simon and W. B. Thompson), Vol. 4, Interscience, New York.
BENFORD G., BOOK D. L. and SUDAN R. N. (1970) *Phys. Fluids* **13**, 2621.
BENFORD G. (1972) *Phys. Rev. Lett.* **28**, 1242.
BENNETT W. H. (1943) *Phys. Rev.* **45**, 890.
ECKER B. (1971) *Bull. Am. Phys. Soc.* **11**, 1249.
FINKELSTEIN D. and STURROCK P. A. (1961) *Plasma Physics* (Edited by J. E. Drummond), Chapter 8, McGraw-Hill, New York.
FURTH H. P. (1963) *Phys. Fluids* **6**, 48.
FURTH H. P., KILLEEN J. and ROSENBLUTH M. N. (1963) *Phys. Fluids* **6**, 459.
HAMMER D. and ROSTOKER N. (1970) *Phys. Fluids* **13**, 1831.
LEARY J. M. and LEE E. P. (1972) *Phys. Fluids* **15**, 716.
LEE K. F. and ARMSTRONG J. C. (1971) *Phys. Rev.* **4A**, 2087, and references therein.
LEE K. F. (1971) *J. appl. Phys.* **41**, 3045.
LONGMIRE C. L. (1967) *Elementary Plasma Physics.* Interscience, New York.
MJOLSNESS R. C. (1963) *Phys. Fluids* **6**, 1730.
PUTNAM S. (1971) *Intense Relativistic Electron Beam-Plasma Interactions in Finite Cavities*, PIIR-29-71, Physics International Company, San Leandro, California. There is also a brief discussion of resistive transverse instabilities herein.
SPENCE P. W., ECKER B. and YONAS G. (1969) *Bull. Am. Phys. Soc.* **14**, 1007.
WEIBEL E. S. (1959) *Phys. Rev. Lett.* **2**, 83.
WEINBERG S. (1967) *J. math. Phys.* **8**, 614.